Statistical Correlation Analysis Between Atmospheric Pollutants Based on Air Quality Monitoring Station Data in Barreiro (Portugal)

João Garcia [1,2,3]

[1] Mechanichal Engineering Department, Instituto Superior de Engenharia de Lisboa, Instituto Politécnico de Lisboa, Lisboa, Portugal
[2] Unit for Innovation and Research in Engineering, Instituto Superior de Engenharia de Lisboa, Instituto Politécnico de Lisboa, Lisbon, Portugal
[3] MARE-Marine and Environmental Sciences Centre/ARNET-Aquatic Research Network, Escola Superior de Tecnologia de Setúbal, Instituto Politécnico de Setúbal, Setúbal, Portugal
Email: joao.garcia@isel.pt

Manuscript received March 5, 2026; revised April 21, 2026; accepted May 7, 2026; published July 20, 2026

***Abstract*—The present study analyses the statistical relationships between atmospheric pollutants and meteorological variables in the municipality of Barreiro (Portugal), based on daily mean data from the local air quality monitoring network. The concentrations of CO, NO_2, SO_2, PM_{10}, and O_3 were considered, as well as meteorological variables including air temperature, relative humidity, wind, and solar radiation. The analysis of linear associations was carried out using the Pearson correlation coefficient. The results show a consistent positive relationship between solar radiation and air temperature (ρ = 0.46 for mean temperature; ρ = 0.55 for maximum temperature), confirming the radiative control of local thermal conditions. PM_{10} particles showed a moderate positive association with temperature (ρ up to 0.30), with a non-linear behavior observed, with higher concentrations both under elevated temperature conditions and in situations of greater atmospheric stability associated with lower temperatures. Ozone showed the most robust meteorological dependence, with a positive correlation with mean temperature (ρ = 0.53) and negative correlations with NO and NO_x (ρ up to −0.58), behavior consistent with photochemical mechanisms and the titration effect in urban environments. Strong correlations were also observed between primary pollutants, namely between CO and NO_x (ρ up to 0.84), reflecting common emission sources associated with road traffic. In contrast, SO_2 showed generally weaker associations with the remaining pollutants. Overall, the identified correlation structure highlights the combined influence of urban emission sources and meteorological conditions on air quality dynamics, contributing to a better understanding of interactions between pollutants in the urban-metropolitan context.**

***Keywords*—air quality, atmospheric pollutants, statistical correlation, meteorological variables, urban environment**

I. Introduction

Atmospheric pollution remains one of the main environmental risks to human health and ecosystems, being responsible for millions of premature deaths per year globally [1, 2]. In urban settings, exposure to pollutants such as nitrogen dioxide (NO_2), carbon monoxide (CO), sulphur dioxide (SO_2), inhalable particles (PM_{10}) and tropospheric ozone (O_3) is associated with the worsening of respiratory and cardiovascular diseases, as well as impacts on vegetation and materials [3]. The complexity of their dynamics results from the interaction between emission sources, chemical transformations in the atmosphere, and local and regional meteorological conditions. At the European level, air quality monitoring and management are framed by Directive 2008/50/EC, currently undergoing revision for alignment with the most recent recommendations of the World Health Organization [4]. In Portugal, the coordination of the monitoring network is ensured by the Portuguese Environment Agency, through the QualAr platform, which provides validated data from air quality stations [5]. These systems constitute the empirical basis for statistical analyses of trends and relationships between pollutants.

Recent scientific literature has highlighted the importance of understanding the interrelationships between atmospheric pollutants and meteorological variables, particularly in the context of climate change and interannual variability [3, 6]. O_3, as a secondary pollutant, results from photochemical reactions involving NO_x and volatile organic compounds under the influence of solar radiation, with positive correlations with temperature and radiation and negative correlations with NO and NO_x commonly observed [7]. In turn, primary pollutants such as CO and NO_x frequently show high correlations with each other in environments dominated by road traffic, reflecting common emission sources [8]. Inhalable particles (PM_{10}) result from both direct emissions and secondary and resuspension processes, being strongly influenced by meteorological conditions such as atmospheric stability, wind speed and relative humidity [9].

Recent studies based on urban time series demonstrate that temperature and solar radiation can enhance secondary particle formation and intensify pollution episodes during periods of atmospheric stagnation [3]. Statistical analysis using correlation coefficients, such as the Pearson coefficient, continues to be widely used to identify linear associations between atmospheric and meteorological variables, constituting a fundamental step in exploratory and local characterization studies [10]. Despite the growing number of international studies, analysis in specific urban contexts remains essential, as pollutant dynamics are strongly influenced by site-specific factors such as urban morphology, proximity to industrial sources, traffic intensity and regional climatic conditions [11, 12].

Moreover, localized investigations have shown that spatial configuration, pedestrian mobility patterns and microenvironmental characteristics can significantly affect pollutant concentrations and human exposure, particularly among sensitive populations such as school children [13–15]. These findings reinforce the need for case-specific assessments supported by robust quantitative approaches. In this regard, structured statistical methodologies have been increasingly used to support environmental and engineering analyses by improving interpretability and inference in complex systems [16]. The municipality of Barreiro, located within the Lisbon Metropolitan Area and historically influenced by industrial and port-related activities, presents relevant characteristics for investigating the relationships between atmospheric pollutants and meteorological variables under a distinct urban-industrial setting.

Within this framework, the present study aims to analyze the statistical correlations between daily concentrations of CO, NO_2, SO_2, PM_{10}, and O_3 and meteorological variables in Barreiro. The intention is to identify patterns of association between pollutants, assess the influence of meteorological conditions on their variability and contribute to a deeper understanding of the physicochemical mechanisms that govern air quality in urban environments.

Although the analyzed data correspond to a period prior to the current reality, their use is justified by the availability of complete, homogeneous and validated time series for the set of pollutants considered, ensuring statistical robustness and methodological consistency. In particular, the analysis of particulate matter focuses on PM_{10} due to the availability of consistent and validated measurements for the study period, whereas $PM_{2.5}$ data were not systematically available across all monitoring stations, which would compromise the comparability of the results. Furthermore, the study period corresponds to a phase still marked by a relevant combination of emission sources, allowing the characterization of the correlation structure between pollutants under a regime representative of the local urban-industrial dynamics.

Notably, the central objective of this work focuses on the analysis of statistical interrelationships between atmospheric variables, rather than on the assessment of absolute pollution levels, which may vary over time. It should be noted that the analysis is based on data from the year 2010, selected due to the availability of complete, consistent and validated time series for all the atmospheric pollutants and meteorological variables considered. Although more recent data could reflect current air quality conditions, such datasets are often affected by gaps, changes in monitoring configurations or differences in measurement methodologies, which may compromise comparability and statistical consistency. In this context, the use of a homogeneous dataset ensures the robustness of the correlation analysis performed. Furthermore, the selected period corresponds to a stage in which the municipality of Barreiro still exhibited a relevant combination of emission sources, particularly industrial and traffic-related, allowing the identification of representative relationships between pollutants and meteorological variables under a well-defined urban–industrial regime. Importantly, the main objective of this study is to analyze statistical interrelationships between variables rather than to assess absolute pollution levels, which may evolve over time.

II. Case Study

The municipality of Barreiro is located in the district of Setúbal, on the southern bank of the Tagus River estuary, facing Lisbon, and is part of the Lisbon Metropolitan Area. It covers approximately 33–34 km², has predominantly flat terrain and is part of the Tagus River basin, factors that may influence atmospheric dispersion processes. The municipality has a high motorization rate, with road traffic currently being the main potential source of atmospheric emissions. Although historically associated with strong industrial activity, Barreiro has experienced a marked decline in its industrial base in recent decades and now presents a predominantly residential character, with significant commuter mobility to Lisbon supported by regular river connections. These characteristics make the municipality a relevant case study for analyzing atmospheric pollutant dynamics in a metropolitan urban context.

A. Atmospheric Pollution Sources

The main sources of atmospheric pollution in Barreiro are associated with road traffic and, to a lesser extent, with industrial activity located in its industrial zone. These components represent the main potential contributions to local atmospheric emissions. The characterization of atmospheric pollution is based on data from air quality monitoring stations integrated into the national network and made available through the QualAr platform [5]. These data allow the assessment of concentration levels of regulated pollutants and support the identification of emission-related patterns.

B. Air Quality Context

Air quality in Barreiro has historically been influenced by the combined effect of industrial activity and road traffic. During the period under analysis, some industrial units with relevance in terms of emissions were still in operation, including a cogeneration plant, inorganic chemistry and fertilizer production units, and other chemical industry facilities. Additionally, the presence of steel-making activity in the neighboring municipality of Seixal represents a potentially relevant regional emission source. The historical industrial presence contributed to exceedances of sulphur dioxide (SO_2) limit values in the Lisbon and Tagus Valley Region. Currently, with the reduction of heavy industry, road traffic has become increasingly relevant, particularly with respect to inhalable particles (PM_{10}). The characterization of air quality is based on data from the national monitoring network, allowing the assessment of pollutant concentrations and their temporal behavior. A summary is presented in Table 1.

Table 1. Summary characterization of PM_{10} concentrations in 2010 [5]

Station	Alto Seixalinho	Escavadeira	Fidalguinhos	Lavradio
Environment type	Traffic	Industrial	Background	Industrial
Annual Mean hourly basis (μg/m³)	33.5	22.0	23.9	23.6
Annual Mean daily basis (μg/m³)	33.6	22.0	23.9	23.6
Annual Maximum hourly basis (μg/m³)	164.6	149.9	178.7	125.4
Annual Maximum daily basis (μg/m³)	106.5	80.1	115.2	105.2

C. Meteorological Context

The meteorological characterization of the study area provides essential context for understanding atmospheric dispersion and transport processes. The analysis is based on data from the Lavradio meteorological station, selected due to its location in an area of industrial influence and the availability of complete and consistent data series. Given the small territorial extent of Barreiro and its predominantly flat morphology, this station is considered representative of local meteorological conditions. The data correspond to the climatological normals provided by the Portuguese Institute for the Sea and Atmosphere [17]. Table 2 presents the general characteristics of the station. The meteorological parameters considered include mean annual temperature, total precipitation, relative humidity, number of days with precipitation above 10 mm, fog occurrence, cloud cover, and frost days, which are relevant for characterizing atmospheric conditions affecting pollutant behavior. Table 3 presents monthly temperature values, including mean, maximum, minimum, and extreme values. Table 4 presents wind frequency and intensity by direction.

Table 2. General characteristics of the Lavradio meteorological station [17]

Station	Latitude N	Longitude W	Altitude (m)
Lavradio	38º41′	9º03′	6

The meteorological characterization of the study area was based on a set of key parameters recorded at the Lavradio station, including mean annual air temperature, total annual precipitation, and relative humidity. Additional variables considered include the number of days per year with precipitation exceeding 10 mm, which provides an indication of intense rainfall events, as well as the frequency of fog occurrence, associated with atmospheric moisture and visibility conditions. Cloud cover at 9 a.m., expressed on a scale from 0 to 10, was also analyzed as an indicator of radiative conditions influencing atmospheric processes. Finally, the number of frost days per year was included to characterize cold weather conditions that may affect atmospheric stability and pollutant dispersion.

Table 3 presents the monthly temperature values measured by this station, with the columns referring respectively to mean temperature, mean maximum temperatures, mean minimum temperatures, absolute maximum temperature in the period considered, and absolute minimum temperature in the period considered.

Table 3. Temperatures measured at the Lavradio station [17]

Month	T_{MED} (°C)	Mean T_{MAX} (°C)	Mean T_{MIN} (°C)	T_{MAX} Abs (°C)	T_{MIN} Abs (°C)
Jan.	10.8	14.5	7.1	20.5	−1.5
Feb.	12.1	15.7	8.6	22.2	0.6
Mar.	13.2	17.5	9.0	26.0	1.4
Apr.	14.9	19.2	10.6	28.5	0.0
May	17.1	21.6	12.7	35.0	3.5
Jun.	20.1	25.1	15.2	37.0	5.0
Jul.	22.4	27.8	17.3	38.5	11.0
Aug.	22.7	28.1	17.3	37.5	10.0
Sep.	21.4	26.6	16.3	37.5	8.5
Oct.	18.0	22.5	13.5	32.0	3.5
Nov.	14.0	17.9	10.2	25.1	0.8
Dec.	11.4	15.2	7.7	24.5	−0.5
Year	16.5	21.0	12.1	38.5	−1.5

Table 4 presents the monthly wind values recorded at the Lavradio station. The columns refer respectively, for each direction (N, NE, E, SE, S, SW, W and NW), to the frequency of occurrence and mean wind speed. The last column presents the frequency of calm conditions (speed below 1 knot).

Table 4. Wind intensity and frequency values collected at the Lavradio station [17]

Month	N		NE		E		SE		S		SW		W		NW		CALM
	FR	VM	FR	VM	FR	VM	FR	VM	FR	VM	FR	VM	FR	VM	FR	VM	FR
Jan.	8.5	10.1	16.4	11.0	3.3	7.5	11.8	8.7	7.2	12.4	17.6	11.7	5.8	10.4	16.4	12.6	13.0
Feb.	9.4	9.8	13.4	9.8	1.3	5.4	11.8	10.8	7.7	14.0	19.9	14.4	5.6	9.7	23.2	13.9	7.6
Mar.	12.6	12.2	13.9	9.0	3.0	6.8	5.2	12.0	4.4	10.4	16.9	12.1	5.6	10.6	34.0	14.2	4.5
Apr.	11.2	11.1	12.6	12.4	2.3	7.9	5.8	12.3	3.6	13.6	14.9	12.7	7.9	11.1	38.6	16.2	3.0
May	11.2	12.3	6.4	10.9	0.9	8.1	3.0	13.0	3.0	16.2	18.2	13.4	7.6	12.0	48.0	15.6	1.5
Jun.	11.8	12.6	6.8	9.2	0.6	12.4	2.7	10.9	2.4	12.0	17.8	12.1	6.6	11.8	50.5	14.3	0.8
Jul.	17.1	12.1	6.1	9.0	1.2	5.0	0.7	10.2	1.3	11.9	12.8	12.0	5.4	11.5	53.0	14.0	2.4
Aug.	16.0	13.1	6.3	10.1	1.2	4.4	1.4	9.5	0.7	13.7	9.2	12.0	4.7	11.1	58.5	14.5	2.0
Sep.	10.5	11.3	11.9	8.1	1.4	4.6	6.0	8.6	3.0	12.2	16.8	12.2	8.8	9.8	37.8	13.1	4.0
Oct.	9.7	10.5	15.6	8.2	1.9	10.6	10.0	9.2	6.3	11.3	14.6	10.3	6.6	9.9	24.4	12.0	10.9
Nov.	15.0	12.3	23.4	10.2	2.6	7.4	10.6	10.4	3.9	10.9	9.9	9.3	4.5	8.2	19.1	12.7	11.2
Dec.	13.4	10.9	22.2	10.2	3.1	6.5	8.6	10.3	4.9	13.9	12.7	12.3	3.7	8.6	15.6	12.1	15.6
Year	12.2	11.7	12.9	9.9	1.9	7.1	6.4	10.3	4.0	12.6	15.1	12.2	6.1	10.5	35.1	14.1	6.3

N: north; NE: northeast; E: east; SE: southeast; S: south; SW: southwest; W: west; NW: northwest; FR: Frequency (%); VM: Mean speed (km/h).

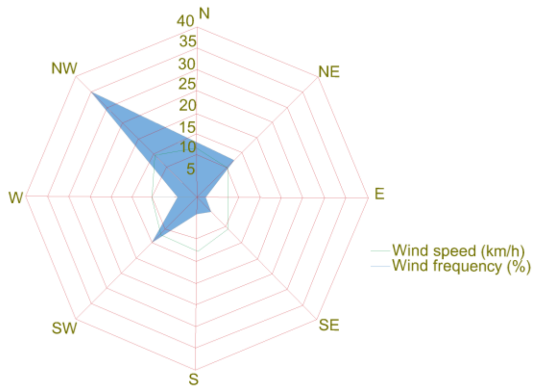

Fig. 1. Wind rose of the Lavradio meteorological station.

Fig. 1 presents the Wind Rose of the Lavradio station. From the analysis of the figure, it can be seen that the prevailing wind direction is NW (frequency 35.1%). The highest wind speeds recorded correspond to the prevailing NW direction (14.1 km/h) and the South direction (12.6 km/h). NW winds are particularly frequent in the summer months (June, July, and August), with the maximum value occurring in August (58.5%). For this direction, the minimum frequency values are recorded in December (15.6%). The mean wind speed is relatively constant throughout the year, with the maximum values recorded in April (16.2 km/h) in the NW direction.

III. Materials and Methods

In this study, data for the year 2010 were used, corresponding to atmospheric pollutant concentrations recorded by the stations of the air quality monitoring network located in the municipality of Barreiro. The following regulated pollutants were considered: carbon monoxide (CO), nitrogen dioxide (NO_2), sulphur dioxide (SO_2), inhalable particles (PM_{10}) and tropospheric ozone (O_3). Additionally, meteorological variables with potential influence on pollutant dispersion and transformation were included, specifically air temperature and relative humidity. Whenever available, wind speed and direction data were also considered, given their relevance in atmospheric transport processes. The meteorological data were provided by the Portuguese Institute for the Sea and Atmosphere (IPMA) and/or by the Electric Power Generation Center (CPPE) of Barreiro. The air quality data were obtained through the official monitoring network, ensuring their validation according to the applicable technical and regulatory procedures. The statistical analysis and data treatment were carried out using R [18, 19], SPSS [20] and Microsoft Excel software [21].

A. Data from Air Quality Monitoring Network Stations

The air quality characterization in Barreiro was based on data from the official air quality monitoring network integrated into the Lisbon and Tagus Valley Region. In 2010, four stations were in operation in the municipality—Alto do Seixalinho, Escavadeira, Fidalguinhos and Lavradio—belonging to the regional network, ensuring representative coverage of the different urban settings. The stations carry out continuous measurements of the main regulated pollutants, namely nitrogen dioxide (NO_2), ozone (O_3), sulphur dioxide (SO_2), inhalable particles (PM_{10}) and carbon monoxide (CO). Air samples are continuously collected through automatic sampling systems and analyzed by standardized instrumental methods, based on physicochemical principles specific to each pollutant (e.g., optical or physicochemical methods). The signals generated by the analyzers are converted into digital values and stored as hourly means, which form the basis for subsequent statistical treatment. In the case of particles, daily means were also considered, in accordance with applicable regulatory procedures. The data are subject to validation and quality control processes before their integration into the official database. Table 5 presents the general characterization of the monitoring network in 2010, including station classification and measured pollutants, while Table 6 summarizes the analytical methods used for the determination of concentrations.

Table 5. General characterization of the Barreiro air quality monitoring network in 2010 [5]

Station	Code	Type of Influence	Address	Parish	Latitude (1)	Longitude (1)	Altitude
Lavradio	3055	Industrial	Rua Vital Pereira	Lavradio	189418	120323	31
Escavadeira	3095	Industrial	Esc.Prep. Mendonça Furtado	Barreiro	188477	118887	30
Alto do Seixalinho	3098	Traffic	Av.Esc.Fuzileiros Navais	Alto do Seixalinho	186964	119039	9
Fidalguinhos	3103	Background	Rua Américo da Silva Marinho	Lavradio	187532	120182	24

(1): Military gauss coordinates.

Table 6. Characterization of analytical methods for pollutants measured at Barreiro air quality stations in 2010 [5]

Station	NO_2	CO	O_3	SO_2	PM_{10}	C_6H_6
Lavradio	Chemiluminescence	NM	NM	Ultraviolet Fluorescence	Beta attenuation	NM
Escavadeira	Chemiluminescence	NM	Photometry	Ultraviolet Fluorescence	Beta attenuation	NM
Alto do Seixalinho	Chemiluminescence	Non-dispersive Infrared Absorption	NM	NM	Beta attenuation	Gas Chromatography with a Photoionization Detector (GC-PID)
Fidalguinhos	Chemiluminescence	Non-dispersive Infrared Absorption	NM	NM	Beta attenuation	NM

NM: Not Measured

It should be noted that, within the scope of the restructuring of the air quality monitoring network of the Lisbon and Tagus Valley Region, the Fidalguinhos station was decommissioned after 2010, according to information provided by the managing entity. However, for the period under analysis, its data were considered relevant for the characterisation of air quality in the municipality. The classification of the network stations—specifically as traffic, background or industrial stations—was defined by the network managing entity, in accordance with European Commission guidelines for the location and classification of air quality monitoring stations. This classification is fundamental for data interpretation, since it allows the distinction between concentrations directly influenced by specific local sources (e.g., road traffic) and levels representative of urban or regional background pollution. In particular, the Fidalguinhos station, classified as a background station, is of particular importance in establishing baseline pollutant concentration levels, minimally influenced by direct local sources. Its location was selected to reduce the immediate influence of emission sources, ensuring greater representativeness of average urban conditions under different meteorological regimes. Fig. 2 presents the location of the air quality stations existing in the municipality during the study period, as well as the stations subsequently decommissioned.

B. Variables and Parameters Considered

In this study, atmospheric and meteorological variables with potential influence on urban air quality dynamics were considered. The atmospheric variables included the concentrations of the analyzed pollutants, obtained from the official air quality monitoring network. Regarding the meteorological variables, air temperature and relative humidity were considered, as well as, whenever available, wind speed and direction, given their relevance in atmospheric dispersion and transport processes. These data were provided by the Portuguese Institute for the Sea and

Atmosphere (IPMA) and/or by the CPPE of Barreiro. Table 7 presents the description of the analyzed variables, including unit of measurement, temporal resolution and type of aggregation used in the statistical treatment.

Fig. 2. Location of air quality monitoring stations in Barreiro (adapted from Google Earth).

Table 7. General description of the variables under study

Variable	Unit	Variable Description
VEL (IM)	(km/h)	Daily mean wind speed
DIREC		Daily prevailing wind direction
TEMP	(°C)	Daily mean temperature
TEMPMAX	(°C)	Daily maximum temperature
TEMPMIN	(°C)	Daily minimum temperature
HUM	(%)	Humidity at 9 a.m. (method used by IM for calculating mean humidity)
HUMmax	(%)	Humidity at 6 a.m. (method used by IM for calculating maximum humidity)
Rad	(watt/m^2)	Daily total radiation
SO_2 med	(μg/m^3)	Daily mean across all stations
NO med	(μg/m^3)	Daily mean across all stations
NO_2 med	(μg/m^3)	Daily mean across all stations
NO_x med	(μg/m^3)	Daily mean across all stations
PM_{10} med	(μg/m^3)	Daily mean across all stations
CO (max) med	(μg/m^3)	Daily maximum value of the 8 h rolling mean, i.e., the 8 h rolling mean was calculated resulting in a mean per hour based on the preceding 8 h. The maximum for that day was then obtained from the 8 h means.
O_3 (max) med	(μg/m^3)	Daily maximum value of the 8 h rolling mean, i.e., the 8 h rolling mean was calculated resulting in a mean per hour based on the preceding 8 h. The maximum for that day was then obtained from the 8 h means.
CO (peak) med	(μg/m^3)	Daily maximum value, without considering 8 h rolling means
O_3 (peak) med	(μg/m^3)	Daily maximum value, without considering 8 h rolling means
NO_x (peak) med	(μg/m^3)	Daily maximum value
SO_2 hos	(μg/m^3)	Daily mean value from the Hospital station
NO hos	(μg/m^3)	Daily mean value from the Hospital station
NO_2 hos	(μg/m^3)	Daily mean value from the Hospital station
NO_x hos	(μg/m^3)	Daily mean value from the Hospital station
CO (max) hos	(μg/m^3)	Daily maximum value of the 8 h rolling mean, from the Hospital station
O_3 (max) hos	(μg/m^3)	Daily maximum value of the 8 h rolling mean, from the Hospital station
CO (peak) hos	(μg/m^3)	Daily maximum value from the Hospital station
O_3 (peak) hos	(μg/m^3)	Daily maximum value from the Hospital station
NO_x (peak) hos	(μg/m^3)	Daily maximum value from the Hospital station
SO_2 lav	(μg/m^3)	Daily mean value from the Lavradio station
NO lav	(μg/m^3)	Daily mean value from the Lavradio station
NO_2 lav	(μg/m^3)	Daily mean value from the Lavradio station
NO_x lav	(μg/m^3)	Daily mean value from the Lavradio station
PM_{10} lav	(μg/m^3)	Daily mean value from the Lavradio station
CO (max) lav	(μg/m^3)	Daily maximum value of the 8 h rolling mean, from the Lavradio station
CO (peak) lav	(μg/m^3)	Daily maximum value of the 8 h rolling mean, from the Lavradio station
NO_x (peak) lav	(μg/m^3)	Daily maximum value from the Lavradio station
NO cam	(μg/m^3)	Daily mean value from the Câmara station
NO_2 cam	(μg/m^3)	Daily mean value from the Câmara station

NO_x cam	(μg/m^3)	Daily mean value from the Câmara station
CO (max) cam	(μg/m^3)	Daily maximum value of the 8 h rolling mean, from the Câmara station
CO (peak) cam	(μg/m^3)	Daily maximum value from the Câmara station
NO_x (peak) cam	(μg/m^3)	Daily maximum value from the Câmara station
SO_2 pai	(μg/m^3)	Daily mean value from the Paio Pires station
NO pai	(μg/m^3)	Daily mean value from the Paio Pires station
NO_2 pai	(μg/m^3)	Daily mean value from the Paio Pires station
NOx pai	(μg/m^3)	Daily mean value from the Paio Pires station
CO (max) pai	(μg/m^3)	Daily maximum value of the 8 h rolling mean, from the Paio Pires station
O_3 (max) pai	(μg/m^3)	Daily maximum value of the 8 h rolling mean, from the Paio Pires station
CO (peak) pai	(μg/m^3)	Daily maximum value from the Paio Pires station
O_3 (peak) pai	(μg/m^3)	Daily maximum value from the Paio Pires station
NO_x (peak) pai	(μg/m^3)	Daily maximum value from the Paio Pires station
SO_2 esc	(μg/m^3)	Daily mean value from the Escavadeira station
NO esc	(μg/m^3)	Daily mean value from the Escavadeira station
NO_2 esc	(μg/m^3)	Daily mean value from the Escavadeira station
NO_x esc	(μg/m^3)	Daily mean value from the Escavadeira station
PM_{10} esc	(μg/m^3)	Daily mean value from the Escavadeira station
CO (max) esc	(μg/m^3)	Daily maximum value of the 8 h rolling mean, from the Escavadeira station
O_3 (max) esc	(μg/m^3)	Daily maximum value of the 8 h rolling mean, from the Escavadeira station
CO (peak) esc	(μg/m^3)	Daily maximum value from the Escavadeira station
O_3 (peak) esc	(μg/m^3)	Daily maximum value from the Escavadeira station
NO_x (peak) esc	(μg/m^3)	Daily maximum value from the Escavadeira station

Table 8 presents the descriptive statistics of the meteorological variables and atmospheric pollutant concentrations analyzed in the present study, including the number of observations (observ.), mean, standard deviation, minimum and maximum values, range, coefficient of variation and, median.

Table 8. Descriptive statistics of the collected variables

Variable	No. Observ.	Mean	Standard Deviation	Minimum Value	Maximum Value	Range	Coeff. of Variation	Median
VEL(IM)	730	4.87	6.58	0	40.5	40.5	1.35	3.1
DIREC	717	4.81	2.74	1	8	7	0.57	6
TEMP	721	17.7	4.48	7.7	31.0	23.3	0.25	17.4
TEMP max	721	22.15	5.78	9.1	40.0	30.9	0.26	21.6
TEMP min	721	14.16	4.06	0.0	26.0	26.0	0.29	14.1
HUM	723	71.93	18.26	6.8	99.1	92.3	0.25	68.0
HUM max	711	84.71	12.58	39.3	99.1	59.8	0.15	87.6
Rad	153	5092.25	1778.02	697.0	7098.0	6401.0	0.35	5802.0
SO_2 med	641	12.61	12.26	1.0	88.6	87.6	0.97	8.4
NO med	641	13.98	15.39	1.1	136.1	135.1	1.10	9.1
NO_2 med	641	29.98	11.94	5.8	72.5	66.7	0.40	28.5
NO_x med	641	48.94	27.92	9.1	188.9	179.8	0.57	42.8
PM_{10} med	617	38.04	21.88	3.5	152.5	148.9	0.58	31.7
CO (max) med	641	491.52	367.15	167.6	2684.1	2516.5	0.75	362.8
O_3 (max) med	641	68.73	25.63	4.2	169.7	165.5	0.37	68.3
CO (peak) med	641	668.09	505.69	195.0	3740.5	3545.5	0.76	503.5
O_3 (peak) med	641	81.79	29.88	6.7	241.3	234.7	0.37	79.0
NO_x (peak) med	641	88.78	54.91	9.0	452.8	443.8	0.62	79.4
SO_2 hos	604	8.52	9.66	1.0	107.6	106.6	1.13	5.5
NO hos	608	14.42	15.71	0.9	129.5	128.6	1.09	9.4
NO_2 hos	608	31.47	14.95	3.7	94.0	90.3	0.48	30.3
NO_x hos	595	50.27	29.90	5.8	230.0	224.2	0.59	43.8
CO (max) hos	634	530.21	410.18	111.6	2972.8	2861.1	0.77	393.8
O_3 (max) hos	619	63.58	27.41	2.0	170.9	168.9	0.43	64.5
CO (peak) hos	640	745.56	617.92	113.0	4075.0	3962.0	0.83	554.0
O_3 (peak) hos	632	77.61	33.07	3.0	260.0	257.0	0.43	74.5
NO_x (peak) hos	595	124.39	91.35	10.0	767.0	757.0	0.73	104.0
SO_2 lav	405	31.34	39.72	1.0	243.1	242.1	1.27	17.1
NO lav	436	8.89	11.39	1.0	100.6	99.6	1.28	5.0
NO_2 lav	438	28.67	14.29	6.6	114.2	107.6	0.50	26.5
NO_x lav	438	41.55	26.19	6.7	205.3	198.6	0.63	35.4
PM_{10} lav	418	31.79	18.53	5.0	161.1	156.1	0.58	25.9
CO (max) lav	346	399.02	299.84	124.5	2529.0	2404.5	0.75	319.2
CO (peak) lav	390	535.69	409.65	62.0	3222.0	3160.0	0.76	421.0
NO_x (peak) lav	438	89.51	69.46	13.0	606.0	593.0	0.78	74.0
NO cam	435	12.62	17.25	1.0	142.8	141.8	1.37	6.5
NO_2 cam	435	33.94	13.06	5.3	70.7	65.3	0.38	34.2
NO_x cam	435	50.55	27.57	3.0	188.9	185.9	0.55	45.4
CO (max) cam	254	673.03	361.60	78.5	1994.9	1916.4	0.54	596.9
CO (peak) cam	327	820.20	511.80	113.0	3077.0	2964.0	0.62	693.0
NO_x (peak) cam	435	107.82	72.61	3.0	528.0	525.0	0.67	91.0
SO_2 pai	515	6.31	6.83	1.0	71.7	70.7	1.08	4.3
NO pai	377	10.01	13.99	1.0	108.9	107.9	1.40	5.6
NO_2 pai	394	23.72	15.01	1.0	73.9	72.9	0.63	21.3
NO_x pai	377	40.19	31.60	2.0	239.3	237.3	0.79	32.8
CO (max) pai	353	422.18	314.23	110.4	2045.6	1935.3	0.74	349.6

O_3 (max) pai	635	75.39	29.72	4.5	183.4	178.9	0.39	75.3
CO (peak) pai	381	646.23	477.08	23.0	3446.0	3423.0	0.74	532.0
O_3 (peak) pai	639	88.13	34.97	6.0	288.0	282.0	0.40	85.0
NO_x (peak) pai	377	97.70	89.42	2.0	748.0	746.0	0.92	73.0
SO_2 esc	598	12.82	14.61	1.0	116.4	115.4	1.14	8.0
NO esc	481	12.56	12.70	1.0	99.4	98.4	1.01	8.1
NO_2 esc	481	26.88	15.81	3.7	97.7	94.0	0.59	24.7
NO_x esc	481	43.31	28.25	4.9	209.1	204.2	0.65	37.3
PM_{10} esc	611	41.91	24.88	3.5	143.9	140.3	0.59	35.3
CO (max) esc	619	423.37	356.36	105.1	2654.3	2549.1	0.84	299.1
O_3 (max) esc	630	66.56	21.77	6.0	154.9	148.9	0.33	67.5
CO (peak) esc	632	555.72	505.73	115.0	3609.0	3494.0	0.91	374.0
O_3 (peak) esc	639	79.05	25.46	11.0	227.0	216.0	0.32	78.0
NO_x (peak) esc	481	133.73	100.12	11.0	509.0	498.0	0.75	111.0

C. Correlation Analysis and Statistical Significance

The analysis of linear associations between the variables under study was carried out using the Pearson correlation coefficient (ρ) presented in Eq. (1), widely used to quantify the strength and direction of the linear relationship between 2 continuous variables. The ρ coefficient is defined by Karch *et al.* [18]:

$$\rho = \frac{\sum_{i=1}^{n}(x_i - \bar{x})(y_i - \bar{y})}{\sqrt{\sum_{i=1}^{n}(x_i - \bar{x})^2} \times \sqrt{\sum_{i=1}^{n}(y_i - \bar{y})^2}} = \frac{cov(X,Y)}{\sqrt{var(X) \times var(Y)}} \quad (1)$$

where $cov(X, Y)$ represents the covariance between the variables and $var(X)$ and $var(Y)$ are the respective variances.

To assess the statistical significance of the coefficients obtained, the *t*-test associated with the correlation coefficient presented in Eq. (2) was used [17]:

$$t = \frac{r\sqrt{N-2}}{\sqrt{1-r^2}} \quad (2)$$

where r represents the sample correlation coefficient and N is the number of observations. The t value follows a Student's t distribution with N–2 degrees of freedom, allowing the null hypothesis of no correlation ($\rho = 0$) to be tested. For large samples, as in the present study ($N \approx 300$ to 700 observations, depending on the variable and station), the critical values approach those of the standard normal distribution.

IV. Results

This section presents the main statistical results obtained from the analysis of the atmospheric and meteorological variables considered.

Regarding the meteorological variables, the mean annual temperature recorded was 17.7 °C, with mean maximum and minimum values of 22.2 °C and 14.2 °C, respectively, showing moderate variability (coefficient of variation below 0.30). Relative humidity had a mean of 71.9%, with a significant range between 6.8% and 99.1%. Wind speed showed high relative dispersion with Coeff. of Variation (CV = 1.35), reflecting the occurrence of occasional intense wind episodes. Regarding atmospheric pollutants, high variability was observed in SO_2, NO, and NOx concentrations at several stations, with coefficients of variation frequently exceeding 1, indicating strong temporal heterogeneity and the occurrence of high concentration episodes. NO_2 showed more moderate variability (CV typically between 0.38 and 0.63), suggesting greater relative stability compared to other primary pollutants. PM_{10} particle means ranged from approximately 31 to 42 µg/m³ across different stations, with coefficients of variation close to 0.6, reflecting the influence of both local sources and meteorological conditions. Carbon monoxide showed a wide range of values, particularly in peak records, with coefficients of variation frequently exceeding 0.75, highlighting the strong influence of traffic-related episodes. Ozone (O_3), analyzed in maximum and peak values, showed moderate variability (CV between 0.32 and 0.43), behavior consistent with its nature as a secondary pollutant dependent on photochemical processes. In general, the comparison between mean and median across several variables indicates right-skewed distributions, particularly for primary pollutants, suggesting the occurrence of occasional high concentration episodes. This characteristic justifies the subsequent correlation analysis and the careful interpretation of statistical results.

Fig. 3 presents the relationship between daily mean temperature and daily solar radiation. A positive overall trend is observed, showing an increase in mean temperature with increasing solar radiation. The Pearson correlation coefficient obtained was $\rho = 0.46$, indicating a moderate positive correlation. The 95% confidence interval (0.33–0.58) excludes the null value, confirming the statistical significance of the association.

This result is consistent with the determining role of solar radiation in the surface energy balance and in the heating of the lower atmospheric layer, constituting a fundamental meteorological factor in the interpretation of relationships between atmospheric variables and pollutant concentrations.

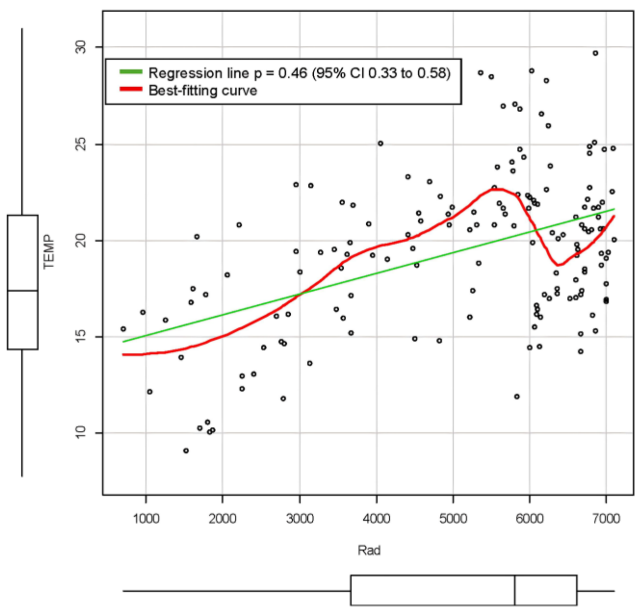

Fig. 3. Mean temperature vs radiation.

Fig. 4 presents the relationship between daily maximum temperature and daily solar radiation. A well-defined positive trend is observed, showing an increase in maximum temperature with increasing solar radiation. The fitted linear regression line visually confirms this association. The Pearson correlation coefficient obtained was $\rho = 0.55$ (95% CI: 0.42–0.64), indicating a moderate to strong and statistically significant positive correlation. Compared to the relationship between radiation and mean temperature, the association with maximum temperature is more intense, which is physically consistent, given that daily maximum values are more directly influenced by the intensity of incident radiation. Despite the dispersion observed for high radiation values—possibly associated with variability in atmospheric circulation or cloud cover—the overall pattern remains clearly increasing. These results reinforce the determining role of solar radiation in daily thermal variability and justify its consideration in the analysis of relationships between meteorological variables and atmospheric pollutant concentrations.

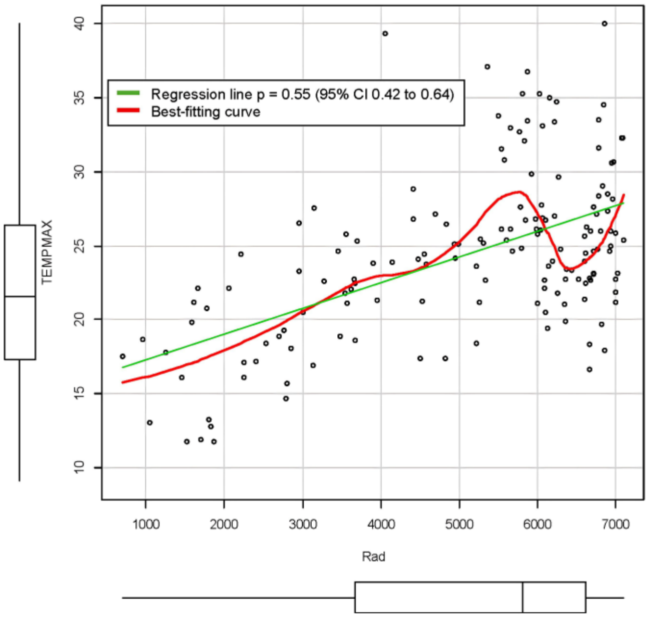

Fig. 4. Maximum temperature vs radiation.

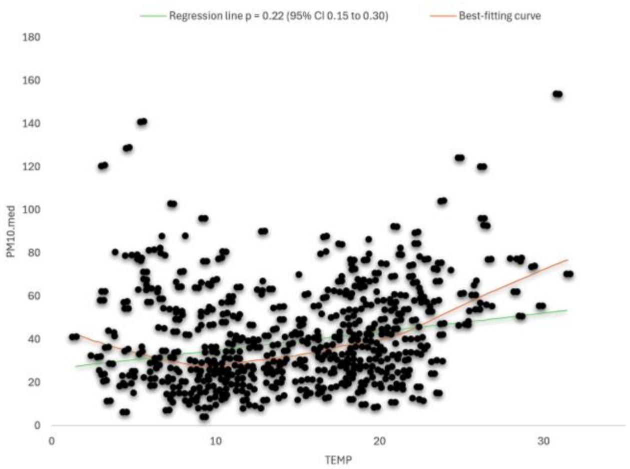

Fig. 5. Mean particle concentration vs mean temperature.

Fig. 5 shows the relationship between daily mean PM_{10} concentration and daily mean temperature. The scatter of points reveals high variability of concentrations across practically the entire thermal range, confirming the weak intensity of the linear association ($\rho = 0.22$; 95% CI: 0.15–0.30). The linear regression line shows a positive slope, but the smoothing curve suggests a non-linear behavior. A slight decrease in concentrations is observed for intermediate temperatures (≈13–17 °C), followed by a progressive increase for temperatures above approximately 20 °C. For temperatures below approximately 13 °C, a tendency for increasing concentrations is also observed, which may be associated with conditions of greater atmospheric stability and reduction in mixing layer height, favoring particle accumulation.

Fig. 6, which represents daily mean PM_{10} concentration as a function of daily maximum temperature, shows a similar pattern but with a slightly more intense association ($\rho = 0.30$; 95% CI: 0.23–0.37). The fitting curve shows a more pronounced increase in concentrations for maximum temperatures above approximately 25 °C, which may be related to particle resuspension processes and secondary aerosol formation under conditions of greater warming. In both cases, the high data dispersion indicates that temperature alone explains only a limited fraction of PM_{10} concentration variability, with the joint influence of other meteorological and emission factors being expected.

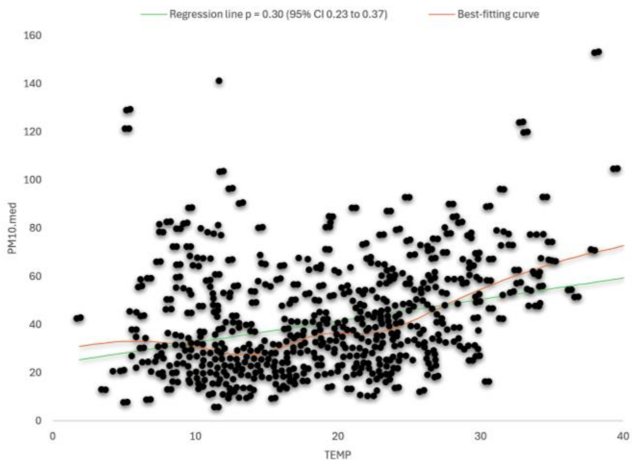

Fig. 6. Mean particle concentration vs maximum temperature.

From the individual analysis by station, it was found that the Lavradio air quality station has the highest correlation coefficient between daily mean temperature and daily mean PM_{10} concentration. Given that the remaining stations show similar patterns but with lower association intensity, only the graph corresponding to the Lavradio station was presented, as it represents the case of greatest statistical relevance in the context of this analysis. This approach allows the observed relationship to be more clearly highlighted, avoiding graphical redundancy and facilitating the interpretation of results.

Fig. 7 presents the relationship between daily mean PM_{10} concentration and daily mean temperature at the Lavradio station. A more evident positive trend is observed compared to the aggregated analysis across stations, confirming that this station shows the strongest association between the 2 variables. The linear regression line shows a positive slope, while the smoothing curve again suggests non-linear behavior, with a slight increase in concentrations for lower temperatures, followed by a more pronounced progressive increase for temperatures above approximately 22–25 °C. This behavior may reflect 2 distinct mechanisms: (i) particle accumulation under conditions of greater atmospheric stability during colder periods, and (ii) increased resuspension and possible secondary aerosol formation under conditions of greater warming. The greater intensity of the correlation observed at this station may be related to its location and to the differentiated influence of local emission sources, as well as to specific characteristics of the ventilation regime in the Lavradio area. These results reinforce the importance of considering analysis by individual station, since spatial aggregation can attenuate locally more expressive statistical relationships.

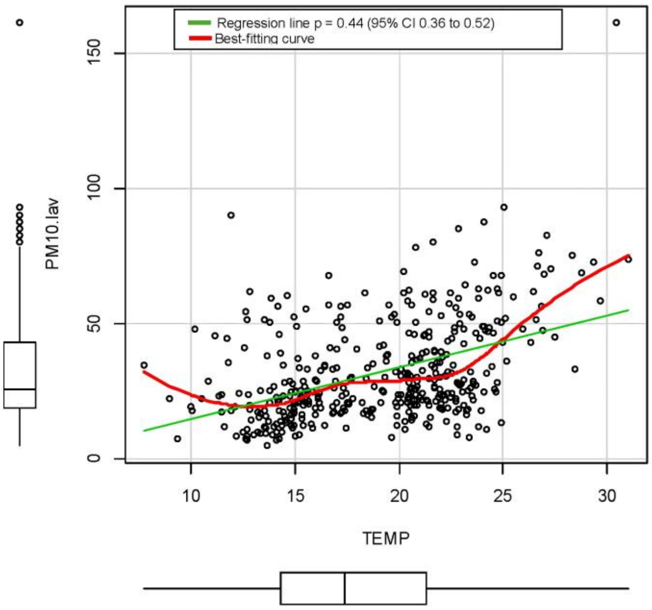

Fig. 7. Particle concentration (Lavradio station) vs temperature.

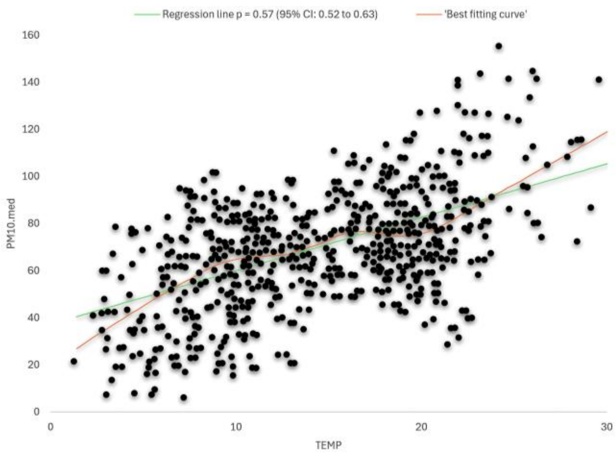

Fig. 8 Maximum ozone concentration (station mean) vs Mean air temperature.

Fig. 8 shows the relationship between the daily maximum O_3 concentration (station mean) and daily mean temperature. A well-defined positive trend is observed across practically the entire thermal range, confirmed by the fitted linear regression line. The smoothing curve suggests a progressive increase in ozone concentrations with increasing temperature, with this increase being particularly evident for temperatures above approximately 20 °C. The scatter of points remains relatively homogeneous across the thermal range, reinforcing the consistency of the association. The Pearson correlation coefficient (ρ = 0.53; 95% CI: 0.47–0.58) indicates a moderate to strong and statistically significant positive correlation. This behavior is physically expected, since tropospheric ozone formation results from photochemical processes dependent on solar radiation and temperature, which accelerate the reactions between NOx and volatile organic compounds. The magnitude of the observed association suggests that temperature constitutes one of the main meteorological factors governing the variability of maximum O_3 concentrations in the study period.

Fig. 9 presents the relationship between the daily maximum O_3 concentration and daily mean temperature at the Hospital air quality station. A well-defined positive trend is observed across the entire thermal range, with a progressive increase in ozone concentrations as temperature rises. The Pearson correlation coefficient obtained (ρ = 0.57; 95% CI: 0.52–0.63) confirms a moderate to strong and statistically significant positive association, slightly higher than that found in the aggregated analysis across stations. The smoothing curve shows a more pronounced increase in concentrations for temperatures above approximately 22–25 °C, suggesting intensification of photochemical processes under conditions of greater warming. The greater magnitude of the correlation at this station may be associated with its station type and lower direct influence of NO emission sources, which promote ozone titration in the immediate vicinity of heavy traffic routes. Thus, the Hospital station may more clearly reflect the regional behavior of O_3 dependent on meteorological conditions. These results reinforce the importance of temperature as an explanatory variable for the variability of maximum ozone concentrations in the urban context studied.

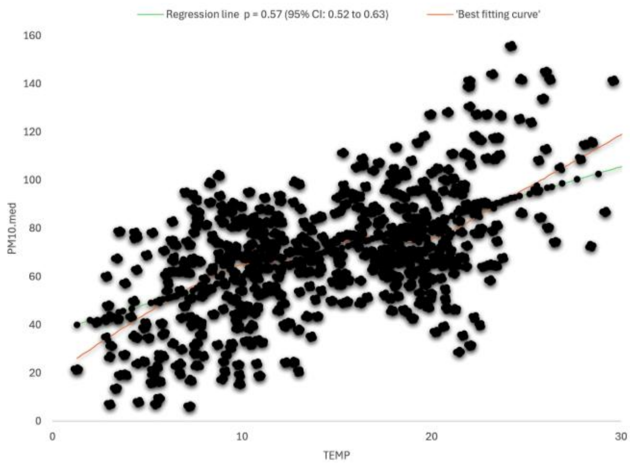

Fig. 9. Maximum ozone concentration (Hospital air quality station) vs Mean air temperature.

Table 9 presents the Pearson correlation (ρ) values between the various variables related to pollutant concentrations, considering the values averaged across all stations (global).

The analysis firstly shows very high correlations between mean and peak values for the same pollutant. Of note are ρ = 0.91 for CO, ρ = 0.95 for O_3 and ρ = 0.85 for NOx (mean vs peak values), revealing strong interdependence between these metrics. This result indicates that the temporal structure of concentrations is consistent regardless of the indicator used, allowing the conclusion that subsequent analyses would not be substantially altered if mean or maximum values were considered.

Table 9. Pearson correlations (ρ) between pollutants

SO_2 med	NO med	NO_2 med	NOx med	PM_{10} med	CO (máx)	O_3 (máx)	CO (pico)	O_3 (pico)	NOx (pico)
1.00									
−0.11	1.00								
−0.01	0.52	1.00							
−0.07	0.90	0.80	1.00						
0.29	0.36	0.47	0.46	1.00					
−0.23	0.82	0.54	0.80	0.39	1.00				
0.36	−0.58	−0.12	−0.46	0.18	−0.50	1.00			
−0.21	0.84	0.59	0.84	0.38	0.91	−0.48	1.00		
0.42	−0.47	0.02	−0.31	0.28	−0.40	0.95	−0.38	1.00	
0.07	0.72	0.69	0.85	0.41	0.66	−0.31	0.77	−0.18	1.00

A. Relationships between Primary Pollutants

In an overall assessment, high correlations are observed between primary pollutants associated with combustion processes. The strong correlations between CO and the NOx families (NO, NO_2 and NOx) stand out, as follows:

$\rho = 0.82$ (maximum CO with mean NO),
$\rho = 0.80$ (maximum CO with mean NOx),
$\rho = 0.84$ (peak CO with mean NO),
$\rho = 0.77$ (peak CO with peak NOx).

These values indicate a close relationship between CO and NOx in urban environments, reflecting their common origin predominantly associated with road traffic [22, 23]. The strong statistical association confirms the internal coherence of the data and the relevance of shared emission sources.

B. Behavior of SO_2

SO_2 generally shows weak correlations with the remaining pollutants, suggesting relatively independent behavior in the analyzed period. The exceptions correspond to the correlations with peak O_3 ($\rho = 0.42$) and maximum O_3 ($\rho = 0.36$), values indicating moderate association. This relationship may reflect common meteorological conditions that simultaneously favor accumulation or regional transport of these pollutants, rather than a direct link between their sources.

C. Relationships Involving PM_{10}

PM_{10} concentrations show moderate correlations with several primary pollutants, as follows:

$\rho = 0.36$ (PM_{10} with mean NO),
$\rho = 0.47$ (PM_{10} with mean NO_2),
$\rho = 0.46$ (PM_{10} with mean NOx),
$\rho = 0.39$ (PM_{10} with maximum CO),
$\rho = 0.38$ (PM_{10} with peak CO),
$\rho = 0.41$ (PM_{10} with peak NOx).

These values suggest that particles are partially associated with the same emission sources as primary gaseous pollutants, namely traffic and combustion [24, 25]. However, the correlations are lower than those observed between CO and NOx, which indicates an additional contribution from other processes, such as dust resuspension, secondary particle formation and regional transport [26]. Regarding ozone, the correlations with PM_{10} are lower ($\rho = 0.28$ for peak O_3 and $\rho = 0.18$ for maximum O_3), showing less direct interdependence between these pollutants. Similarly, the correlation between PM_{10} and SO_2 is relatively weak ($\rho = 0.29$), suggesting limited influence of common sources in the analyzed period. Overall, PM_{10} is found to be correlated with all the analyzed pollutants, showing a stronger association with NO_2 and a weaker one with O_3, which is consistent with the coexistence of primary and secondary components in the particulate fraction.

D. Negative Correlations Involving Ozone

One of the most relevant results of the correlation matrix is the negative association between O_3 and nitrogen oxides, with the following standing out: $\rho = -0.58$ (O_3 with mean NO), $\rho = -0.46$ (O_3 with mean NOx).

This negative relationship is consistent with the atmospheric chemistry of tropospheric ozone. In urban environments, NO acts as a titration agent of O_3, reacting directly with it and temporarily reducing its concentration. Thus, high concentrations of NO tend to be associated with lower levels of O_3, explaining the negative sign of the observed correlation.

In summary, the correlation matrix shows 2 main structural patterns:(i) a group of strongly intercorrelated primary pollutants (CO, NO, NO_2, NOx), associated with urban combustion sources. (ii) ozone, with distinct and partially inverse behavior relative to nitrogen precursors, reflecting its nature as a secondary pollutant dependent on photochemical processes.

V. CONCLUSIONS

The present study allowed the characterization of the correlation structure between atmospheric pollutants and meteorological variables in the municipality of Barreiro, revealing statistically significant patterns consistent with the physicochemical mechanisms described in the literature.

The results confirm the strong thermal dependence associated with solar radiation, with a moderate positive correlation observed between radiation and mean temperature ($\rho = 0.46$) and an even higher one for maximum temperature ($\rho = 0.55$), reflecting the determining role of radiation in the atmospheric energy balance.

Regarding PM_{10} particles, a positive, albeit moderate, association with air temperature was found ($\rho = 0.22$ for mean temperature and $\rho = 0.30$ for maximum temperature). The analysis suggests non-linear behavior, with increasing concentrations both under elevated temperature conditions—possibly associated with resuspension and secondary formation—and at lower temperatures (below approximately 13 °C), a situation consistent with greater atmospheric stability and reduced dispersion.

Ozone showed the most robust association with temperature, presenting a moderate to strong positive correlation with daily mean temperature ($\rho = 0.53$). This result confirms the photochemical nature of O_3 and its dependence on meteorological conditions favorable to the intensification of reactions between NOx and volatile organic compounds.

The analysis of interrelationships between pollutants revealed 2 distinct structural patterns: (i) primary pollutants associated with combustion (CO and NOx) strongly correlated with each other, reflecting common emission sources, namely road traffic; and (ii) ozone, with partially inverse behavior relative to its nitrogen precursors, consistent with the titration effect and urban photochemical dynamics.

These findings contribute to a better understanding of the mechanisms governing urban air quality in mixed urban-industrial environments and highlight the importance of considering meteorological conditions in the interpretation of pollutant behavior.

From an applied perspective, the identified correlation patterns may support air quality management strategies and the development of more effective monitoring and mitigation approaches, particularly in urban areas with similar emission profiles.

Despite the statistical robustness of the correlations obtained, the study has some limitations. Firstly, the analysis was based on simple linear correlations, not allowing the establishment of causal relationships nor the assessment of multivariate interactions between meteorological variables and emissions. Secondly, the use of daily means may attenuate short-duration phenomena and extreme episodes, potentially relevant to urban air quality dynamics. Additionally, factors such as particle chemical composition, real-time traffic intensity or specific regional transport contributions, which could enrich the interpretation of results, were not considered.

As future developments, the application of multivariate statistical models (for example, multiple regression or generalized models) is recommended, which would allow the quantification of the relative contribution of different meteorological and emission variables. The incorporation of seasonal analysis and lagged effects (temporal lags) may also deepen the understanding of the underlying mechanisms, especially in the case of ozone. Additionally, the integration of more recent data and comparison with periods following the restructuring of the local industrial base will allow the assessment of the evolution of the correlation structure over time. Studies linking air quality variables with public health indicators, using appropriate epidemiological methodologies, may further contribute to a more comprehensive assessment of the environmental and social impacts of atmospheric pollution in the urban context.

Conflict of Interest

The author declares no conflict of interest.

References

[1] World Health Organization. WHO global air quality guidelines. [Online]. Available: https://www.who.int/publications/i/item/9789240034228

[2] Health Effects Institute. State of global air 2023. [Online]. Available: https://www.stateofglobalair.org/resources/report/state-global-air-2023

[3] European Environment Agency. Air quality in Europe—2023 report, Luxembourg: Publications office of the European Union, 2023. [Online]. Available: https://www.eea.europa.eu/publications/air-quality-in-europe-2023

[4] European Commission—Environment. Revision of the Ambient air quality directives. [Online]. Available: https://environment.ec.europa.eu/topics/air/air-quality/revision-ambient-air-quality-directives_en

[5] Portuguese Environment Agency. [Online]. Available: https://apambiente.pt/ar-e-ruido/qualidade-do-ar-0

[6] Climate change 2021: The physical science basis. [Online]. Available: https://www.ipcc.ch/report/ar6/wg1/downloads/report/IPCC_AR6_WGI_FrontMatter.pdf

[7] P. S. Monks, C. Granier, S. Fuzzi *et al.*, "Atmospheric composition change—global and regional air quality," *Atmos. Environ.*, vol. 43, no. 33, pp. 5268–5350, 2009.

[8] European Environment Agency, European Union emission inventory report 1990–2021—Under the UNECE convention on long-range transboundary air pollution. [Online]. Available: https://horizoneuropencpportal.eu/sites/default/files/2024-05/eea-european-union-emission-inventory-report-1990-2021-2023_0.pdf

[9] A. Bose and I. R. Chowdhury, "Investigating the association between air pollutants' concentration and meteorological parameters in a rapidly growing urban center of West Bengal, India: A statistical modeling-based approach," *Model. Earth Syst. Environ.*, vol. 9, pp. 2877–2892, 2023.

[10] D. Zhan, M. P. Kwan, W. Zhang *et al.*, "Spatiotemporal variations and driving factors of air pollution in China," *Int. J. Environ. Res. Public Health*, vol. 14, no. 12, 1538, 2017.

[11] B. Augusto, D. Lopes, S. Rafael *et al.*, "Assessing the impact of different urban morphology scenarios on air pollutant emissions distribution," *Sci. Total Environ.*, vol. 950, 175341, 2024.

[12] M. T. Abbasi, A. A. Alesheikh, A. Jafari *et al.*, "Spatial and temporal patterns of urban air pollution in tehran with a focus on $PM_{2.5}$ and associated pollutants," *Sci. Rep.*, vol. 14, 25150, 2024.

[13] J. N. P. M. Garcia, L. M. R. Coelho, C. M. P. Gouveia, *et al.*, "Analyses of human exposure to urban air quality in a children population," *Int. J. Environ. Pollut.*, vol. 40, no. 1-3, pp. 94–108, 2010.

[14] J. Garcia, R. Cerdeira, L. Coelho *et al.*, "Influence of pedestrian trajectories on school children's exposure to PM_{10}," *J. Nanomater.*, vol. 2014, 505649, 2014.

[15] J. Garcia and R. Cerdeira, "Assessing indoor and outdoor PM_{10} levels in school: Insights from a case study," *Int. J. Environ. Sci. Dev.*, vol. 16, no. 3, pp. 225–233, 2025.

[16] N. R. Costa and J. Garcia, "Applying design of experiments to a compression refrigeration cycle," *Cogent Eng.*, vol. 2, no. 1, 992216, 2015.

[17] Portuguese Institute for the Sea and Atmosphere. Climatological normals 1991–2020. [Online]. Available: https://www.ipma.pt/pt/oclima/normais.clima/1991-2020/

[18] J. D. Karch, A. F. Perez-Alonso, and W. P. Bergsma, "Beyond pearson's correlation: Modern nonparametric independence tests for psychological research," *Multivariate Behavioral Research*, vol. 59, no. 5, pp. 957–977, 2024.

[19] The R project for statistical computing. [Online]. Available: https://www.R-project.org/

[20] IBM Corp. IBM SPSS Statistics for Windows, Version 29.0, Armonk, NY: IBM Corp. [Online]. Available: https://www.ibm.com/products/spss-statistics

[21] Microsoft Corporation, Microsoft Excel, Version 365, Redmond, WA: Microsoft Corporation. [Online]. Available: https://www.microsoft.com/microsoft-365/excel

[22] H. Zheng, S. Kong, S. Zhai *et al.*, "An intercomparison of weather normalization of $PM_{2.5}$ concentration using traditional statistical methods, machine learning, and chemistry transport models," *npj Clim. Atmos. Sci.*, vol. 6, 214, 2023.

[23] N. Cholianawati, T. Sinatra1, G. A. Nugroho *et al.*, "Diurnal and daily variations of $PM_{2.5}$ and its multiple-wavelet coherence with meteorological variables in Indonesia," *Aerosol Air Qual. Res.*, vol. 24, 230158, 2024.

[24] H. M. Adly and S. A. K. Saleh, "Long-term trends in PM_{10}, $PM_{2.5}$, and trace elements in ambient air: Environmental and health risks from 2020 to 2024," *Atmosphere*, vol. 16, no. 4, 415, 2025.

[25] E. Manevska, O. Dimitrovska, I. Radevski *et al.*, "Meteorological parameters versus PM10: Statistical analysis of the city of Skopje, Republic of North Macedonia Using multiple linear regression," *Pol. J. Environ. Stud.*, vol. 32, 2023.

[26] M. J. Alam, I. Karim and S. U. Zaman, "Seasonal dynamics and trends in air pollutants: A comprehensive analysis of $PM_{2.5}$, NO_2, CO, SO_2 and O_3 in Houston, USA," *Air Qual. Atmos. Health*, vol. 18, pp. 2625–2642, 2025.